INVESTIGATING THE ADSORPTION OF VOLATILE CORROSION INHIBITORS ONTO Fe, Al and Al 2024 ALLOY IN A SYNTHESIZED ATMOSPHERE OF H_2S AND SO_2

Paul Jaeger
Conditions Inc.

Luis F. Garfias-Mesias and William. H. Smyrl
Corrosion Research Center, Department of Chemical Engineering and Materials Science, University of Minnesota, Minneapolis, Minnesota 55455, USA.

ABSTRACT

Evaporated aluminum and AL 2024 were used to investigate the mass change associated with the adsorption of different Volatile Corrosion Inhibitors (VCIs) by using the Quartz Crystal Microbalance (QCM) and the Scanning Electron Microscope (SEM). Atmospheres containing H_2S, SO_2, H_2SO_4, NH_4Cl and KBr at a Critical Relative Humidity (CRH) of 80 and up to 100% and temperatures between 5 and 50^oC were used to corrode aluminum 2024. The SEM images of the uninhibited 2024 samples revealed a highly corroded surface, whereas the inhibited samples showed less attack after exposure to the aggressive environments. Analysis of the particles within the aluminum matrix showed the VCIs prevented attack of both the matrix and the particles containing Mg, Mn, Fe and Cu, whereas the non-inhibited sample showed partial corrosion of the particles. The QCM data identifies unique adsorption rates and limiting adsorption thresholds. The XPS identifies unique peaks marking adsorption of the inhibitor adsorbed on the surface.

Key words: Aluminum 2024, Al, Quartz Crystal Microbalance, QCM, Scanning Electron Microscopy, SEM, H_2S, SO_2, H_2SO_4, NH_4Cl, KBr, Critical Relative Humidity, CRH, Volatile Corrosion Inhibitors, VCI's, Fe, Mn, Mg, Cu, corrosion, inhibitors, XPS, sodium nitrite, X-ray Photoelectron Spectroscopy, XPS, Atmospheric corrosion

INTRODUCTION

The widespread use of VCIs is gaining acceptance in a number of applications ranging from the petrochemical to the electronics and telecommunications industries. This increase has also increased the interest to study these types of inhibitors in atmospheric and accelerated aggressive test atmospheres. However not much is known or shown how inhibitors protect or even not protect or protect to a lesser degree than another inhibitor on different metals and or their alloys. It is also relatively unknown why different inhibitors or combinations of them protect only certain metals. Benzotriazole, for example, is a very well known inhibitor for copper. However, its protection efficiency fails when it's used to protect iron or steels. Benzoates are another example of inhibitors with multifunctional properties. Ammonium benzoate, for example, is used quite often in industrial applications and has been found, by using the QCM and other techniques, to adsorb on iron providing excellent corrosion protection[1]; it has been also found to be a good inhibitor for aluminum but not copper.

This paper is an understanding of how certain VCIs work and protect certain metals. Most inquiries are on the order of "how" do they work, can you detect them on the surface and to what degree can they protect? To answer these questions first an understanding of inhibitors must be presented. This happens by first understanding the kinetics of adsorption and the affinity towards metals for which they inhibit, and then investigate them using conventional surface analysis like the SEM. Most of the recent studies have used different techniques like SEM-EDS, XPS, Ellipsometry, and other methods to identify the adsorbed films or to analyze the protection to the substrate.

Identification of corrosion begins at the micrometer range since most of the precursor sites for corrosion begin at this level. Analysis of the chemical composition on a metals surface and the identification of precursors for corrosion on the surface (normally particles) is normally done in the micrometer range. The SEM is one of the tools commonly used for this purpose. By mapping the surface of a sample one can analyze and identify different particles before and after an exposure to an aggressive environment. Inhibitors also need to be studied in the micro/nanometer scale since most of the properties offered from an inhibitor are due to an adsorbed layer(s) with thickness in the nanometer range. On this type of a scale, one can definitively determine what type of protection an inhibitor can supply an inhibitor/substrate interaction before and after a test; or most importantly from real life/time exposure.

The Quartz Crystal Microbalance (QCM) has been used to understand VCI adsorption. It has been used to assess the performance of different inhibitors by measuring the adsorption on the surface of an inhibitor from the gas phase.[1,2] The QCM works on the principle of the inverse piezoelectric effect. This effect was discovered by Jaques and Pierre Curie[3] and is the basis by which one measures the oscillations in an ionic crystalline solid when a voltage is supplied to the crystal via evaporated electrodes. *In-situ* changes in the resonance frequency are then recorded when a mass (normally

taken as the increase in crystal thickness) is added to the substrate. This addition of mass is normally very small due to the few absorbed monolayers or chemical reactions with the substrate's surface. As the mass/thickness increases, the relative resonant frequency of the crystal decreases. Normally, piezoelectrics have long been recognized as excellent indicators of mass changes because of the direct relationship between mass change and resonant frequency response. An equation developed by Sauerbrey in 1959 shows the linear relationship between deposited mass and frequency[1] according to the following equation:

$$\Delta f = -2.3x10^{6}\ f^{2}\ m/A$$

Where **Δf** is the change of frequency measured (in Hz), **f** is the resonant frequency given in MHz, **m** is the increment of mass in the substrate and **A** is the area exposed. Therefore, **m/A** is the change in mass deposited on the crystal per unit area (g/cm^2). Equation 1 was originally used by Sauerbrey for a cut crystal vibrating in the thickness shear mode. The ability of the QCM to detect a mass change as small as 10^{-9} grams make it an essential tool for the *in-situ* monitoring of mass changes due to the oxidation and or the adsorption of a substrate at the gas/metal interface. The QCM represents an attractive technique to detect such small changes with high accuracy and to give an estimation of the protective film formed in the surface of most materials. By using the QCM, one can identify the thickness of the film or the rate of oxidation with and without a VCI[1,2]. The rates of corrosion are normally used as the basis for determining the efficiency factor of most VCIs. In a recent study the QCM was used to monitor the reaction of silver in jet fuels containing elemental sulfur and hydrogen sulfide[4], thus showing its ability to assist in the detection of corrosion.

X-ray photoelectron spectroscopy (XPS) is another analytical tool for identifying an adsorbed VCI film. XPS provides one with the ability to detect any changes or additions to a (oxide) film on the surface of a metal. It does this by detecting the change in binding energies, that are normally found, for certain valence states of known elements. Because of this capability XPS can be used to identify any anomalies, if any, in the binding energies of the natural occurring elements found on a metallic/conductive surface.

Very few studies have been undertaken to compare the protection of some commercially available VCIs[1,2], despite the impact of atmospheric corrosion. It is well known that the corrosion rate increases when there is an increase in both the relative humidity and temperature[5]. For aluminum Patterson and Wilkinson[6] have suggested that a critical relative humidity of 80% is needed for corrosion to begin. In addition, it has been established that the concentration of aggressive gases like H_2S and SO_2 in the atmosphere may cause general attack when they are present on the order of 1 to 10 parts per billion (ppb)[7]. Part of the objective of the present work was to identify the protection offered from different inhibitors for aluminum 2024 exposed to concentration levels of H_2S and SO_2 up to 100 PPM. During the exposure time, the CRH

was kept above 80% and the temperature ranged between 5-50^{o}C. Due to the varying temperatures the RH reached 100% at the point of the lowest temperature for a short period of time and then returned to lower values when the temperature was increased to 50^{o}C. This was done with the aim of stimulating the aggressiveness of the corrosive evaporating electrolyte. It was in this accelerated aggressive test that we aimed to show the protection that a VCI can offer to a commercially available grade of an aluminum alloy (Al 2024).

EXPERIMENTAL

Sample Preparation

Al 2024. Commercial Al 2024 samples were polished with SiC paper using polishing oil and going from 600 grit down to 4000 grit, as recommended by Alodan and Smyrl[8]. After finishing the coarse polishing, the samples were respectively polished with 6 and 1 µm diamond paste and oil. After the samples were visually inspected and having obtained a mirror-like finish, they were cleaned using reagent grade isopropanol alcohol (IPA) in an ultrasonic bath followed with a second rinsing of IPA and then a final rinse with 18M ohm deionized (DI) water. Finally, the samples were dried with ultra pure nitrogen.

AT cut quartz crystals (5 MHz resonant frequency) supplied by Valpey-Fisher were cut to achieve a zero temperature coefficient at 25^{o}C. The crystals were then fitted with two key hole type electrodes by means of evaporation using a Varian Electron Beam Evaporator. Three different layers were deposited prior to the experiment. First a 500 Angstrom layer of Ti was evaporated onto the crystal, followed by 1500 Angstroms of Au and finally a 1500 Angstroms of 99.999% pure Al. After completion of the evaporation the crystal was then fitted into a probe made from Kel F® which was inserted into a customized 150 ml, 5 neck, 2 gas inlets glass flask. Details of the cell are described elsewhere[2]. The data acquisition was done using a IEEE board on a personal computer.

Materials

The inhibitors used in this experiment were $(C_6H_{11})_2NH\ NO_2$ (dicyclohexylammonium nitrite or more commonly known as DICHAN), with a melting point of 139^{o}C, sodium nitrite and two proprietary inhibitors which are a blend of amine carboxylates (Supplied by Cortec Corporation). These inhibitors will be referred to as A,B and C throughout the rest of the paper. The reactants used to produce the H_2S and SO_2 and to control the relative humidity were: $Fe_2(SO_4)_3$, $Na_2S_2O_3 \cdot 5H_2O$, H_2SO_4, NH_4Cl and KBr (all reagent grades and obtained from Aldrich Chemical, Milwaukee WS).

Corrosion Tests

The Al 2024 samples were suspended in a 3.8 liter glass container. For each inhibitor two 2024 samples were exposed to the inhibitor followed by the corrosive environment (two control samples were also tested, with no inhibitor added). All the containers with

the samples and the inhibitors (neither the solutions nor the chemicals were placed in the container with the control samples) were then sealed and left for 24 hours at room temperature. After the 24 hour exposure, the glass containers were opened and three petri dishes were placed on the bottom of each container. One of these petri dishes contained a saturated solution of KBr and NH_4Cl in distilled water, needed to maintain the CRH of 80%. The second and third petri dishes contained $Fe_2(SO_4)_3$ and $Na_2S_2O_3 \cdot 5H_2O$ respectively.

The production of the H_2S and SO_2 was accomplished by adding H_2SO_4 into the two petri dishes containing the $Fe_2(SO_4)_3$ and $Na_2S_2O_3 \cdot 5H_2O$. The amount of H_2SO_4 used was obtained from the calculations done previously to attain an estequiometric chemical reaction producing 50-100 PPM H_2S and SO_2 in each respective petri dish. The samples were then left in the sealed jars containing the aggressive environment for 24 hours. During the first 16 hours of exposure, the temperature of the jars was controlled at 20^oC with 80% RH. In the following 4 hours the jars were placed in a convection oven (which average temperature is $50^oC \pm 2$ and RH no less than 80%). This was followed by a 2 hour cooling to 5^o C which increased the RH to 100%. Finally during the last two hours, the jars were removed and heated back to 50^oC and with a RH of no less than 80%. After this cycle, the samples were cleaned in an IPA ultrasonic bath and rinsed with IPA.

Surface analysis.

After the corrosion tests, the Al 2024 samples were analyzed in a SEM (Jeol 840II, with an integrated EDS system) to obtain X-ray mapping and particle analysis. For all the samples, a preliminary examination of a chosen area was done before corrosion testing. Within the selected areas some particles with representative composition among all of them were chosen, identified and analyzed. Then, after the corrosion tests, the same area was located and the same particles previously analyzed were again tested. In all the cases, it was relatively easy to find the areas that had been previously marked.

XPS analysis was completed by using a model PHI 5400 from Physical Electronics Inc., Eden Prairie MN All samples were exposed to a laboratory atmosphere for a minimal amount of time during transfer from the QCM chamber to a desicator and then into the XPS chamber.

RESULTS AND DISCUSSION

Figure 1 shows the SEM micrographs obtained from the control sample before (1a) and after (1b) the exposure. By comparing Figures 1a and 1b we observe that the general attack on the surface is very severe due to the aggressiveness of the test; furthermore, most of the particles have also been. This is seen by the distinct contrast of the light and dark areas and the distinctive irregular shapes. Figure 2 shows the X-ray spectra from

particle (P3), as shown in figure 1, containing Mn, Fe and Cu before (2a) and after the test (2b). It is quite obvious that the relative peaks associated with Mn, Cu and Fe have disappeared. It is also interesting to mention that a new peak, associated with sulfur was found in the sample after the corrosion test. The sulfur is likely to have originated from the exposure to the sulfur-containing condensates. Figure 3 shows similar spectra from particle (P2) found in the same area as shown in Figure 1. This particle contained mainly Cu and Mg. After the test, the Cu was retained (confirmed by the presence of the 3 Cu peaks before and after exposure). However, the Mg had disappeared and the new sulfur peak was present after the test.

The findings may be explained by the fact that Cu is cathodic to Al 2024 and Fe, Mg and Mn are anodic and therefore can be dissolved presumably in low pH solutions such as the condensate. All of the three inhibitors used presented relatively little attack to the surface during the exposure. Figure 4 shows the images of an area which contained some particles similar to those found in the control sample. The difference between Figures 4a and 4b demonstrate that the attack suffered during the exposure was relatively mild, as can be seen by the absence of the large irregular cauliflower like images and the staining. In the samples exposed to the aggressive environment, but inhibited with any of the three inhibitors, it was less difficult to locate the particles which were previously found before the corrosion test. Figures 5a and 5b show the spectrum from particle (P2) as shown in figure 4. This particle mainly contains Mn, Fe and Cu. After the exposure, all the peaks associated with those elements still remained in transient i.e. with the same relative intensities. This gives an indication that the main role of the inhibitors is to protect both the weak sites present in the material, which normally are precursors for localized attack[8], and the Al matrix.

Finally, Figures 6a and 6b show similar results for a Mg-containing particle (image not shown) before and after the test. Notice that the Mg peak together with the Cu peaks remained almost the same after the corrosion test. Another important feature shown in these two spectra is the presence of a very discrete peak of sulfur after the exposure. The relative intensity of this peak contrasted with the ones shown for the control sample where the peak is normally the second largest after Al. This demonstrates the ability of the inhibitor to protect the sample against most of the aggressive components of the corrosive media, particularly sulfur.

The results shown here demonstrate that the main effect of the inhibitors used here is to protect the particles and the matrix from any kind of attack from the aggressive atmosphere. Furthermore, the ability of the inhibitors to decrease the adsorption of sulfur containing species on the surface of the metal can be one of the main reasons by which the metal is protected. The inhibitors investigated here indicate through the SEM observations and the QCM that they provide protection to Al and probably to Al 2024. This is also confirmed by numerous field applications. Further work is in hand to try and find any other relevant effect of the inhibitors and any differences from one to another which can lead to a concise ranking of the effect of such inhibitors. This can be

accomplished by using different techniques like X-ray Photoelectron Spectroscopy (XPS) and Atomic Force Microscopy (AFM) to study the composition of the 'inhibited' layer and its respective thickness.

Figure 7a shows an adsorption plot of dichan on evaporated iron. The plot shows that adsorption ceases after 24 hours. The quick change in frequency indicates a quick adsorption and that adsorption is finite for this inhibitor substrate combination. The graph even shows no desorption, at standard room temperature and pressure, occurring once the source has been removed. Thus, possibly suggesting it is a chemically adsorbed inhibitor under these conditions.

Figure 7b are two independent QCM plots of adsorption from the inhibitor dichan on evaporated aluminum. The plots show a relatively steady decrease in the frequencies once the inhibitor has been introduced into the contained atmosphere. Notice the rate is much slower than on iron. The relative steady rate was monitored over a period of four days and it appears that the adsorption could continue thereafter. This continuous adsorption leads up to the question: Is there an adsorption limit for aluminum like iron and is there a certain 'amount' of inhibitor needed to identify it's presence using XPS? In addition this information could possibly be used to support adsorption bonding order information as obtained by TEM techniques such is the case where K. Cho *et al* found the order for BTA adsorption on copper.

Figure 7c shows a plot of the QCM for the inorganic inhibitor sodium nitrite. Due to its non-volatile nature as a corrosion inhibitor it was as a non-volatile control for the QCM. The QCM plot shows no significant change over the course of the five-day exposure thus indicating its inability to protect from the gas phase.

Figures 8a, b and c are plots of the XPS binding energy results for the O1s peak for iron surfaces. Figure 8a shows the binding energies of atmospheric oxides found on the surface, notice that the peak is fairly symmetric. Figure 8b represents what the surface of iron looks like when exposed to VCIs and the inhibitor dichan in atmospheric conditions. Notice the additional hump in the O1s peak. It is this hump that appears to identify the presence of a chemically adsorbed VCI. Figure 8c does not show the characteristic 'hump' in the O1s peak identifying an adsorbed VCI. This would indicate that the sodium nitrite did not make it to the surface and also supports the QCM data showing no adsorption. Figure 8d, on the other hand, does not support the findings of the SEM micrographs (figures 1-6) nor the QCM data (figures 7a, b, c), when compared to the plot of the binding energies for the same inhibitor on iron. This may be, as the frequency change from the QCM pointed out, that more time is be needed for the inhibitor to adsorb on the aluminum surface. It could also be that dichan adsorbs physically or a weak chemical bond which subsequently would desorb during the vacuum down process during the XPS analysis.

Kuznetsov has shown the adsorption and desorption of multiple inhibitors using ellipsometric techniques and calculated the film thickness changes on iron over time. Figure 9a shows the rapid growth and film thicknesses of five inhibitors. For example, looking at two of the plots in 9a (1) 1-2-aminoethanol and (2) N,N,N-ethyldiethynolamine it is quite clear that (1) has a mostly physical adsorption due it's greater amount of relative desorption to adsorption and (2) appears to share a physical and chemical adsorption as indicated by the relatively smaller amount of desorbed material to that of the adsorbed material. This graph demonstrates that certain inhibitors may not be able to protect a substrate as well if the emitting source is removed from the same enclosed space where the metal is. It also indicates there are varying degrees of adsorption, both physical, as seen in the desorption process, and chemical adsorption as seen by the irreversible desorption.

Figures 9b and c show Kuznetsov's XPS findings for detecting multiple inhibitors on the surface of iron. He has identified a shift in the binding energy of the O1s and Fe2p3/2-electron spectra on the surface of iron as compared to a surface without exposure to the inhibitors. Indications of the inhibitors presence in the XPS indicates that the type of adsorption is most likely chemical due to the extremely low vacuum pressures needed to do the analysis.

CONCLUSIONS

The study of aluminum inhibited with different VCIs was outlined and the two techniques used to investigate the inhibition of different Volatile Corrosion Inhibitors (VCIs) were the QCM and SEM. The QCM clearly indicates the physical effects, an *in situ* frequency change, of adsorption/reaction that lead to the inhibition of corrosion of aluminum. A corrosive atmosphere containing H_2S, SO_2, H_2SO_4, NH_4Cl and KBr at Critical Relative Humidity's (CRH) of no less than 80% and up to 100% was used along with temperatures between 5 and 50^{o}C to simulate extreme conditions for exposure of Al 2024. The SEM imaging of the Al 2024 surface of the non-inhibited samples revealed severe general corrosion, whereas the inhibited samples showed significantly less corrosion. Analysis of the inclusions within the aluminum matrix showed that the addition of the VCIs to the atmosphere protected the inclusion particles (normally containing Mg, Mn, Fe and Cu), whereas in the non-inhibited sample, particles of similar composition corroded. In addition, the Cu inclusions that were inhibited were not attacked in any of the environments. The latter shows that the inhibitor is especially effective in protecting Cu. Cathodic protection of the Cu by the surrounding matrix may also be involved. The surface of the samples was also significantly protected by the presence of the different inhibitors.

Inhibitors adsorbed differently (chemically or physically) on different substrates (iron and aluminum) and different inhibitors can adsorb differently onto one substrate.

XPS confirmed a most probable chemical adsorption of amine based inhibitors on iron surfaces and the QCM and SEM suggest a most probable physical adsorbtion of the ‘dichan’ on aluminum

ACKNOWLEDGMENTS

A grant from the NSF and discussions with Dr. Maher Alodan are greatly acknowledge.

REFERENCES

1. Leng and M. Stratmann *Corros. Sci.* **34,** 1657 (1993)

2. P. Jaeger and W. H. Smyrl, Corrosion/96 Conf. Denver, Co. Paper **626**

3. Applications of Piezoelectric Quartz Crystal Microbalances; Elsevier Science Publisher: 1984

4. Zabarnick S., Zelesnik P., Whitacre S.D. *Ind. Eng. Chem. Res.*, **35**, 2576 (1996).

5. R.E. Lobnig, D.J. Siconolfi, J. Maisano, G. Grundmeier, H. Strekel, R. P. Frankenthal, M. Stratmann, J. D. Sinclair *J. Electrochem. Soc*., Vol.143,No. 4, April 1996

6. W.S. Patterson and J.H. Wilkinson, *J. Soc. Chem. Ind*., **57**, 445 (1938)

7. R. B. Comizzoli, R. P. Frankenthal, R. E. Lobnig, G. A. Peins, L. A. Psota-Kelty, D. J. Siconolfi and J. D. Sinclair, *Interface*, **2**, 26 (1993).

8. M. Alodan and W. H. Smyrl, *J. Electrochem. Soc.* **144**, L282 (1997).

9. Y. I. Kuznetsov, Corrosion 98 Conference San Diego, Ca paper **242**

FIGURES

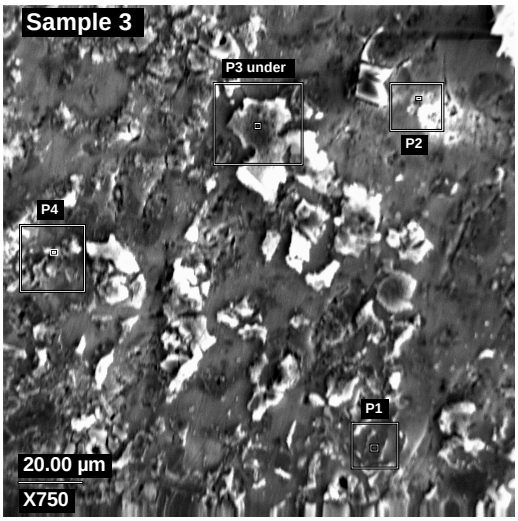

Figure 1

Figure 1 shows a SEM image of Al 2024 (control sample) after the test.

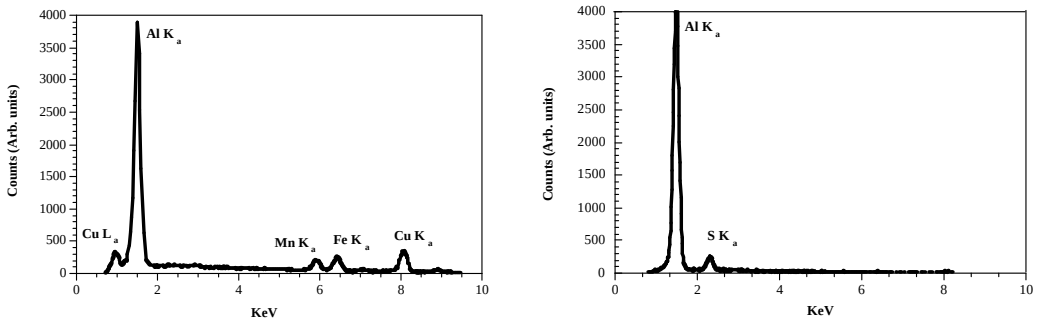

a) **b)**

Figure 2 shows the X-ray spectrum from particle (P3) shown in figure 1. a) before the test and b) after the corrosion test. Notice that the peaks associated with Cu, Mn and Fe disappeared after the test, whereas a new peak related to sulfur appeared.

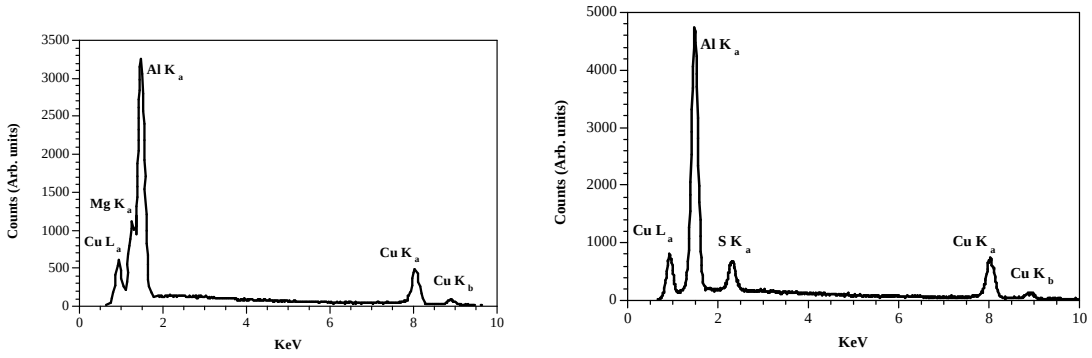

Figure 3 shows the X-ray spectrum from particle (P2) shown in figure 1. a) before the test and b) after the corrosion test. Notice that the peaks associated with Cu still remained after the test contrasting with the Mg peak that had disappeared. Again, a new peak related to sulfur appeared after the test.

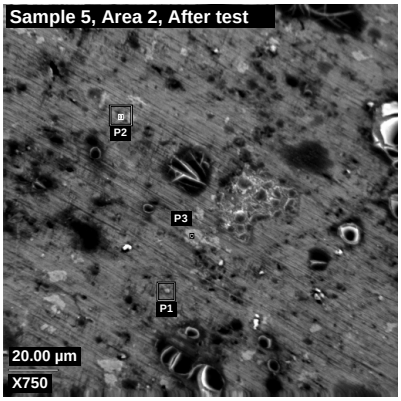

Figure 4

Figure 4 shows a SEM image of an inhibited Al 2024 sample after the test. Notice that the damage suffered due to the exposure of the sample to the aggressive environment is relatively mild.

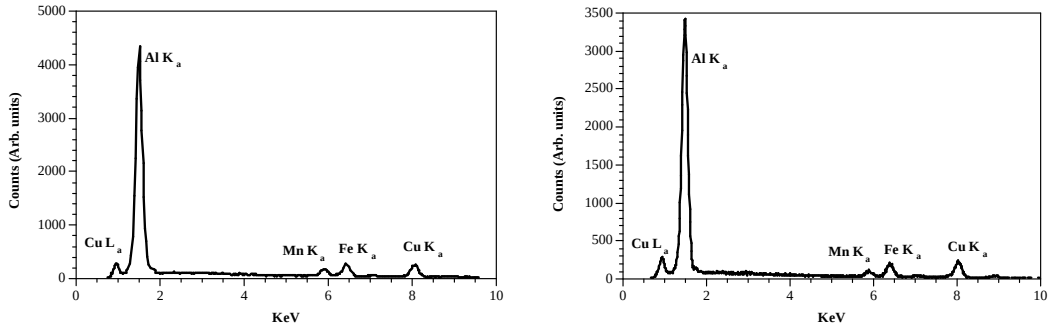

Figure 5 shows the X-ray spectrum from particle (P2) shown in figure 4. a) before the test and b) after the corrosion test. Notice that the peaks associated with Cu, Mn and Fe still remained after the test .

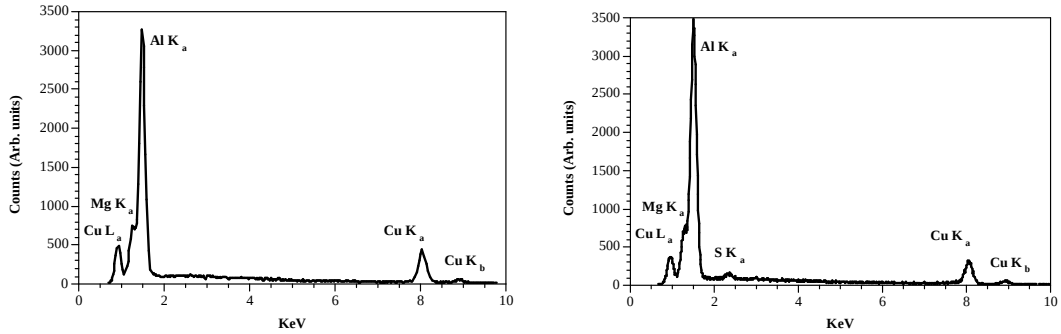

Figure 6 shows the X-ray spectrum from a Mg inclusion in an inhibited sample of Al 2024; a) before the test and b) after the corrosion test. Notice that the relatives peaks associated with Cu and Mg still remained after the test. Again, a new peak related to sulfur appeared after the test.

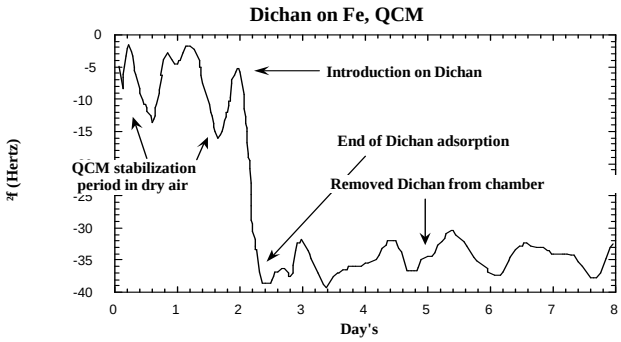

Figure 7a. QCM data showing a mass increase (as seen from the decreasing frequency) on the surface of iron caused by adsorption of dicyclohexylammonium nitrite

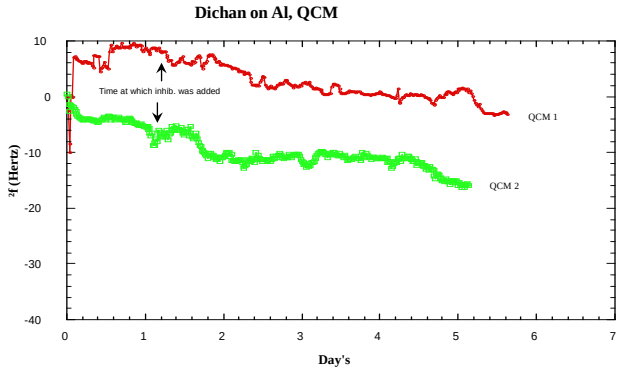

Figure 7b QCM data showing a mass increase (as seen from the decreasing frequency) on the surface of aluminum caused by adsorption of dicyclohexylammonium nitrite

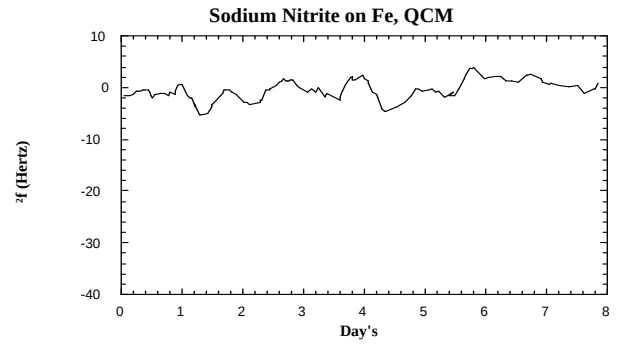

Figure 7c QCM data showing no mass increase or decrease on the surface of iron when influenced by sodium nitrite in the gas phase

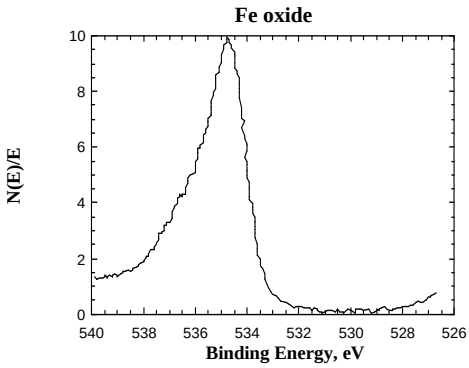

8a

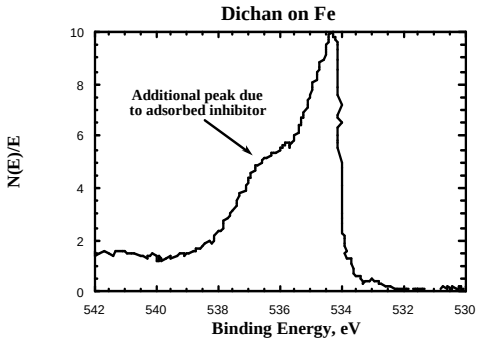

8b

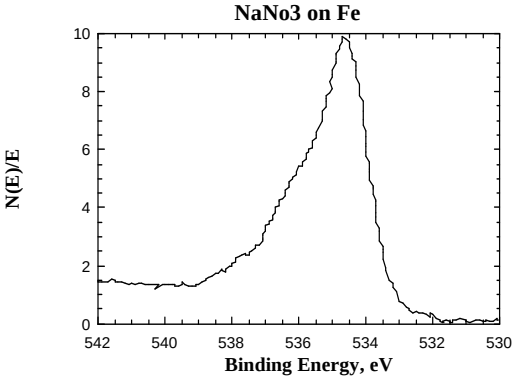

8c

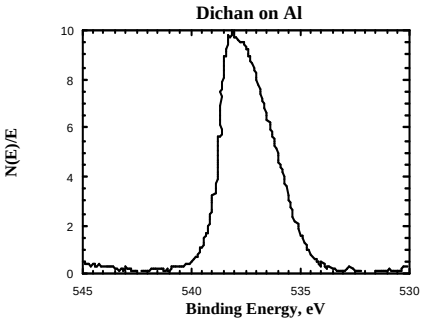

8d

Figures 8a, b, c and d showing the binding energies of evaporated metal surfaces exposed to VCIs. 8a shows the surface of iron exposed to atmospheric conditions. 8b represents the surface of iron exposed to dichan and VCIs in atmospheric conditions. 8c shows the surface of iron exposed to sodium nitrite vapors in atmospheric conditions. 8d shows the surface of aluminum exposed to dichan in atmospheric conditions

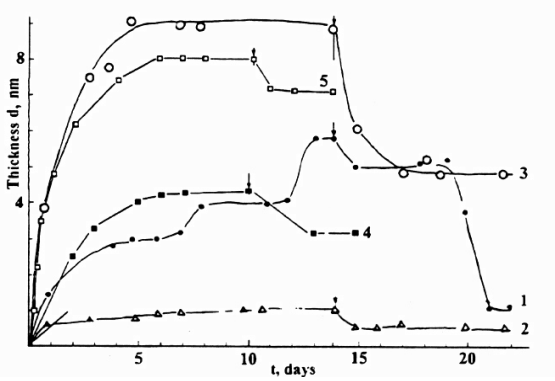

Figure 8a Kuznetsov's plot of adsorbed/desorbed VCI film thickness on iron over time: 1. 2-aminoethanol; 2. N, N, N-diethylaminolamine; 3. N, N-diethylaminoethanol; 4. N, N-diethylaminopropionitrile; 5. 1-diethylamino-2-methyl-butanone-3. The arrows mark the time at which the VCI source was removed. Note the change in the plot indicating desorption of the film.

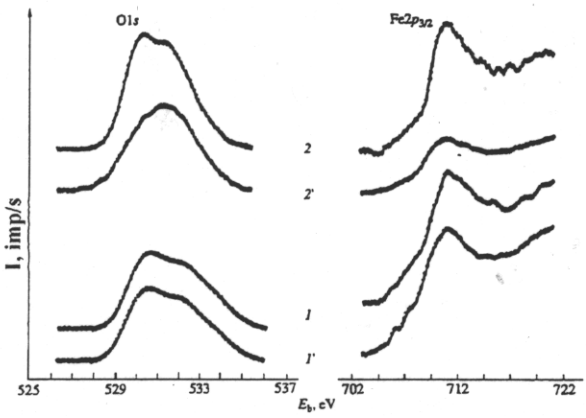

Figure 8b Kuznetsov's plot showing the O1s and Fe2p3/2 peaks on iron from exposure to DEAPN vapors (1, 1') for 30 hours and (2, 2') for 300 hours. Note: 1' and 2' are after washing in ethyl alcohol.